Single-Bit Digital Frequency Synthesis via Dithered Nyquist-rate Sinewave Quantization

Paul P. Sotiriadis, *Senior Member, IEEE* , Natalia Miliou, *Member, IEEE*

Abstract—Single-Bit Nyquist-rate quantization of sinewaves with random dithering is studied as a means for all-digital frequency synthesis. Quantizer's output spectrum is analytically derived and related to the cumulative distribution function of the random dither formed by independent and identically distributed random variables. Necessary and sufficient conditions for spurs-free output are derived. The noise floor level due to random dithering is derived analytically and the output dynamic range is defined. The trade-off between selective frequency-spurs presence and dynamic range improvement is studied. Several MATLAB examples illustrate the theory and its applications.

Index Terms—Clock generation, digital-to-analog converter, digital-to-frequency converter, direct digital synthesis, frequency spurs, quantization.

I. INTRODUCTION

Over the past few years the interest in digital-intensive and all-digital frequency synthesis has been revitalized due to the challenges in traditional analog-RF design caused by the reduced power supply voltage and co-integration with digital engines in standard-CMOS processes [1]-[29]. Moreover digital-intensive frequency synthesizers are benefited by the automated design, verification and layout tools available for digital circuits, and can be migrated to newer IC technologies with less effort than their traditional analog counterparts [2].

Direct Digital Synthesizers (DDS) [31]-[33] and All-Digital Phase-Locked Loops (ADPLL) [2] are the two dominant digital-intensive frequency synthesis architectures with many applications and realizations. Despite their success and impact on modern IC design, both of them require critical analog and mixed signal blocks like the Digital to Analog Converter (DAC) of the DDS, the Time-to-Digital Converter (TDC) and the Digital Control Oscillator (DCO) of ADPLL.

Eliminating these last mixed-signal/analog blocks in frequency synthesizers implies the extreme requirement of generating *single-bit* digital signals of desirable *sinewave-like* spectrum using only a digital circuit with a reference clock. Efforts towards this can be traced at least thirty years back [34]-[36]. Recent developments in this direction include a number of architectures [12]-[30] most of which focus primarily on generating variable-frequency clock signals for clocking other digital circuits [12]-[22]. Techniques for generating RF signals with relatively clean spectrum include [24]-[29] and they use additional retiming blocks, cleanup-PLLs and dithering methods, where only some of the last ones are purely digital.

In addition to the design and implementation advantages of a completely digital RF frequency synthesizer, a synchronous single-bit digital signal which can be used as the carrier or local-oscillator signal in an RF chain has also certain advantages: A) It can be amplified, for transmission or internal use, without distortion and with very high efficiency using a switching amplifier; B) It can be used directly, without the need of a limiter or comparator, to drive a switching up- or down–converting frequency mixer; C) It can be easily fed to some phase detectors or related blocks for synchronization purposes.

Digital phase and frequency modulation of a synchronous single-bit digital signal with sinewave-like spectrum can be easily achieved when the signal is generated by certain all-digital synthesizers [24]. Amplitude modulation can also be implemented using a Look-Up-Table (LUT) or by linearly combining two or more such signals [2], [24]. More complex modulation schemes result from combinations of the above.

This work studies in detail the spectral properties of synchronous single-bit digital signals generated by single-bit, dithered Nyquist-rate quantization of sinewaves. In practice, such signals are generated using a phase accumulator followed by a sinewave LUT whose output is additively dithered and quantized to single bit. This is the same with having a DDS with a 1-Bit Nyquist-rate DAC[1] and amplitude dithering. Since a 1-Bit DAC is a comparator or simply a Most Significant Bit (MSB) truncator, this approach results in direct all-digital frequency synthesis architectures without a DAC at the output and without the need for oversampling.

Considering signal quantization from a frequency-synthesis perspective, the paper focuses on a special case of the general quantization theory [37]-[38] providing a deep analysis on the relationship between dithering and spectral content. The main results of the paper are listed in the table below.

The spectrum of dithered single-bit quantized sinewave as a function of the dither's distribution	Theorem 1
Necessary and sufficient conditions for dither's distribution for *spurs-free* spectrum.	Theorem 2
The trade-off between frequency-spurs present and dynamic range improvement.	Example 5

Table 1: Main results of the paper

Starting in Section II the use of dithering is shown to be unambiguous in single-bit quantization for RF frequency synthesis. Section III defines the mathematical tools and

[1] clocked by the DDS' clock; *not* an oversampling DAC [45]

introduces the Chebyshev polynomial series expansion of the dither's cumulative distribution function.

Two main results of the paper are captured in Theorems 1 and 2 in Sections IV and V respectively. Specifically, Section IV derives analytically the spectrum of the dithered signal providing the frequency locations and amplitudes of all frequency components and the noise floor power level. Section V provides necessary and sufficient conditions for spurs-free output and introduces a metric of the output's dynamic range illustrating a trade-off between the dynamic range and selectively acceptable frequency spurs. Finally, Section VI provides the concluding remarks.

II. Un-Dithered Single-Bit Sinewave Quantization

One way to generate a synchronous single-bit digital signal is to use a DDS with a 1-Bit Nyquist-rate output DAC, where the DAC essentially acts as a comparator[2]. This crude quantization is by far the dominant source of frequency spurs at the output compared to the sinewave representation errors introduced by any reasonably-sized LUT. The scheme is practically equivalent to that in Fig. 1 of single-bit sinewave quantization where the Zero-Order-Hold (ZOH) function captures the behavior of the 1-Bit DAC.

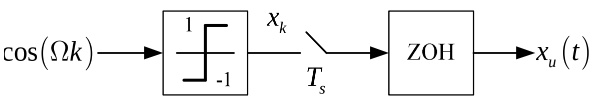

Figure 1: Undithered single-bit quantization of a sinewave

In Fig. 1 we have $x_u(t) = \sum_{k=-\infty}^{\infty} \operatorname{sgn}(\cos(\Omega k)) \cdot p(t/T_S - k)$ where T_S is the sampling period and p is the ZOH function

$$p(t) = \begin{cases} 1 & \text{if } t \in [0,1) \\ 0 & \text{otherwise} \end{cases} . \qquad (1)$$

Then the Fourier transform of $x_u(t)$ can be expressed as

$$X_u(f) = W(f) \cdot \sum_{k,m=-\infty}^{\infty} \frac{(-1)^m}{2m+1} \delta\left(f - \frac{2m+1}{T_S}\frac{\Omega}{2\pi} - \frac{k}{T_S} \right) \qquad (2)$$

where $W(f) = (2/\pi) e^{-i\pi T_S f} \operatorname{sinc}(T_S f)$ is a weighting function with $\operatorname{sinc}(a) = \sin(\pi a)/(\pi a)$ for $a \neq 0$ and $\operatorname{sinc}(0) = 1$. For all practical purposes it is $\Omega = 2\pi w / q$.

<u>Assumption:</u> Throughout the paper w, q are positive integers satisfying $0 < w < q/2$.

Replacing $\Omega = 2\pi w / q$ in (2) it can be concluded that the set of frequency tones at the output $x_u(t)$ is $\left\{ \frac{1}{T_S} \cdot \frac{w + \ell \cdot \gcd(2w, q)}{q} \middle| \ell \in \mathbb{Z} \right\}$. Therefore the output is full of (strong) spurs for most values of Ω with very few exceptions. Fig. 2 shows a typical case of the spectrum. The output signal is unusable for most applications due to the density and strength of spurs, this motivates the use of dithering.

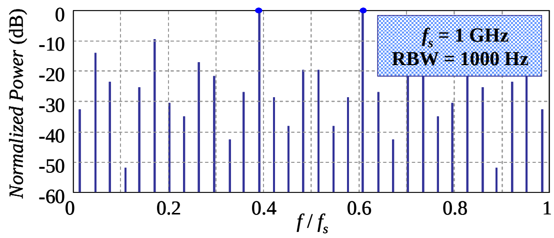

Figure 2: Spectrum of *undithered* single-bit-quantized sinewave with $w = 25$, $q = 64$ and $f_s = 1/T_S$; derived ignoring the weighting function $W(f)$. The strongest frequency components are at frequencies $\Omega/(2\pi T_S)$ and $1/T_S - \Omega/(2\pi T_S)$.

<u>Remark 1</u>: Motivation for using dithering in the quantization of the sinewave is gained by comparing the spectrum in Fig. 2 to the one in Fig. 7 achieved with the dithering methodology described in the following sections. Another pair of spectra of undithered and dithered single-bit quantized sinewave where $w = 5831$ and $q = 2^{18}$ is shown in Fig. 3 and Fig. 15.

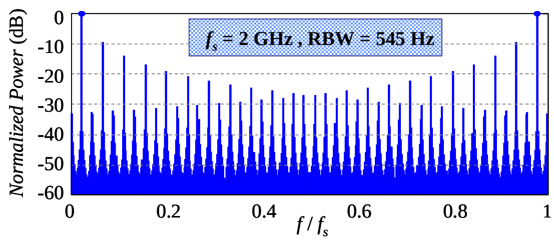

Figure 3: Spectrum of undithered single-bit quantized sinewave with $w = 5831$, $q = 2^{18}$ and $f_s = 1/T_S$, ignoring weighting factor $W(f)$.

III. Dithered Single-Bit Sinewave Quantization

Dithering is used widely to suppress the spurs and shape the noise spectrum of quantization in DDS [31] and in data converters in general [44]. Single-bit quantization without oversampling [45], as in Fig. 4, is an extreme case. Yet, we show that using random dithering $\mathbf{u}_k$ of appropriate statistics we can eliminate all spurs, or, keep some of them selectively to allow for lower noise floor (introduced by the dither).

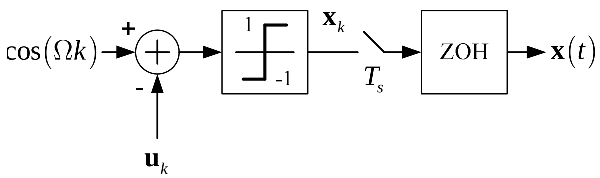

Figure 4: Dithered single-bit quantization of a sinewave

A. *Definitions, Notation and Assumptions*

Dithered single-bit quantization is shown in Fig. 4. The random sequence $\{\mathbf{u}_k\}$ is subtracted from the sinewave resulting in the discrete-time signal $\mathbf{x}_k = \operatorname{sgn}(\cos(\Omega k) - \mathbf{u}_k)$ which is written more explicitly as

[2] or simply keep only the MSB of the LUT's output assuming an appropriate numerical representation is used.

$$\mathbf{x}_k = \begin{cases} 1 & \text{if} \quad \mathbf{u}_k < \cos(\Omega k) \\ -1 & \text{if} \quad \mathbf{u}_k > \cos(\Omega k) \\ 0 & \text{otherwise} \end{cases} \tag{3}$$

Although dithering sequences $\{\mathbf{u}_k\}$ with any statistical properties can be used, those with Independent and Identically Distributed (IID) random variables are easier to generate in hardware, mathematically tractable and can achieve complete spurs elimination as demonstrated in the following sections.

<u>Assumption:</u> Sequence $\{\mathbf{u}_k\}$ is formed of IID random variables with Cumulative Distribution Function (CDF) $G:[-1,1]\to[0,1]$ which is continuous and has continuous first and second derivatives[3] in $[-1,1]$, i.e. $G\in C^2([-1,1])$.

We use this assumption from here on and so for every $k\in\mathbb{Z}$ and $u\in[-1,1]$ it is $\Pr(\mathbf{u}_k \le u) = G(u)$.

Eq. (3) implies that the random variables $\{\mathbf{x}_k\}$ are also independent (to each other) but not identically distributed. Specifically it is

$$\begin{aligned} \Pr(\mathbf{x}_k = 1) &= G(\cos(\Omega k)) \\ \Pr(\mathbf{x}_k = -1) &= 1 - G(\cos(\Omega k)) \end{aligned} \tag{4}$$

Note that if $\Omega/(2\pi)$ is rational, i.e. $\Omega = 2\pi w/q$, which is always true in practice, $\{\mathbf{x}_k\}$ is cyclostationary (in the strict sense) [39] of period $q/\gcd(q,w)$. Finally, the output signal of the quantizer is the continuous-time stochastic process

$$\mathbf{x}(t) = \sum_{k=-\infty}^{\infty} \mathbf{x}_k\, p\left(\frac{t}{T_S} - k\right) \tag{5}$$

where $p(t)$ is the ZOH function in Eq. (1). Using the integer part function "$[\,\cdot\,]$", Eq. (5) can also be written as

$$\mathbf{x}(t) = \mathbf{x}_{[t/T_S]} \;. \tag{6}$$

The Power Spectral Density (PSD) of a Wide-Sense Stationary (WSS) process $\mathbf{x}(t)$ is the Fourier transform of its autocorrelation function [39]. Sequence $\{\mathbf{x}_k\}$ however is not WSS and neither the continuous-time stochastic process $\mathbf{x}(t)$ is. Therefore we have to employ the more general average-autocorrelation function for $\mathbf{x}(t)$, defined as

$$\overline{R}_X(t) \triangleq \lim_{L\to\infty} \frac{1}{2L} \int_{-L}^{L} R_X(t+\tau,\tau)\, d\tau \tag{7}$$

where $R_X(t_1,t_2) = E\{\mathbf{x}(t_1)\mathbf{x}(t_2)\}$ is the autocorrelation function. Then the PSD of $\mathbf{x}(t)$ is defined via the Fourier transform

$$S_x(f) = \int_{-\infty}^{\infty} \overline{R}_X(t)\, e^{-2\pi i f t}\, dt \tag{8}$$

[3] There exist milder but more technical conditions sufficient for the validity of our analysis especially taking into account the monotonicity of G [41][48].

Note that when $\Omega = 2\pi w/q$, the stochastic process $\mathbf{x}(t)$ is cyclostationary and (7) reduces to the corresponding definition in [39]. Finally, the discrete-time average-autocorrelation function of the random sequence $\{\mathbf{x}_k\}$ is defined similarly as

$$\overline{r}_x(k) \triangleq \lim_{M\to\infty} \frac{1}{2M+1} \sum_{m=-M}^{M} r_x(k+m,m) \tag{9}$$

where $r_x(n,m) = E\{\mathbf{x}_n \mathbf{x}_m\}$ is its autocorrelation function. Definition (9) is identical to that used in [40] except that the averaging here is bilateral.

IV. PSD of Dithered Single-Bit Quantized Sinewave

The spectral properties of the continuous-time stochastic signal $\mathbf{x}(t)$ are inherited from those of the discrete-time random signal $\{\mathbf{x}_k\}$. This is shown by the more generally applicable Lemma 1 whose proof is in the Appendix.

<u>Lemma 1</u>: *Let $\{\mathbf{x}_k\}$ be a real random sequence with bounded autocorrelation function r_x and average autocorrelation function $\overline{r}_x$. Also let $p(t)$ be given by Eq.* (1). *Then the PSD of the random process $\mathbf{x}(t) = \sum_{k=-\infty}^{\infty} \mathbf{x}_k\, p(t/T_S - k)$ is*

$$S_x(f) = T_S \cdot \mathrm{sinc}^2(f T_S) \cdot s_x(2\pi f T_S) \tag{10}$$

where $s_x(\omega) = \sum_{k=-\infty}^{\infty} \overline{r}_x(k) e^{-ik\omega}$ is the Discrete-Time Fourier Transform (DTFT) *of the average autocorrelation function $\overline{r}_X$ and $T_S \cdot \mathrm{sinc}^2(f T_S)$ is due to the shape of pulse $p(t)$*[4]. □

To derive a closed form expression of the dithered single-bit quantized sinewave spectrum using (10) we calculate first the discrete-time average autocorrelation function $\overline{r}_X(k)$. To do so it is convenient to express the CDF $G:[-1,1]\to[0,1]$ as a series of Chebyshev polynomials of the first kind, i.e.,

$$G(u) = \frac{1}{2} + \frac{1}{2}\sum_{j=0}^{\infty} a_j T_j(u) \tag{11}$$

where the $1/2$ summand and multiplying factor simplify the algebraic manipulation to follow. The coefficients a_j are derived based on the orthogonality properties [41] of Chebyshev polynomials according to

$$a_0 = \frac{2}{\pi}\int_{-1}^{1} \frac{G(u)}{\sqrt{1-u^2}}\, du - 1\,, \quad a_{j>0} = \frac{4}{\pi}\int_{-1}^{1} \frac{G(u) T_j(u)}{\sqrt{1-u^2}}\, du \tag{12}$$

Our assumption that $G\in C^2([-1,1])$ guaranties that series expansion (11) converges to G everywhere in $[-1,1]$, [41]. Reversely, we can define G using coefficients a_j but we must verify that G is indeed a CDF. The two equations and the inequality in (13) form a necessary and sufficient set of conditions for G to be a CDF.

[4] Eq. (10) can be modified accordingly for other shapes of $p(t)$.

$$G(-1)=0, \quad G(1)=1 \quad \& \quad G'(u)\ge 0 \quad \forall u\in[-1,1] \qquad (13)$$

Since it is $T_j(1)=1$ and $T_j(-1)=(-1)^j$ for $j=0,1,2,\ldots$, and $T_j'(u)=j\cdot U_{j-1}(u)$ for $j=1,2,3,\ldots$, where U_j is the j^{th} Chebyshev polynomial of the 2$^{\text{nd}}$ kind [41], Eqs. (13) become

$$\begin{array}{l} \sum_{j=0}^{\infty}(-1)^j a_j=-1, \quad \sum_{j=0}^{\infty}a_j=1 \\ \sum_{j=1}^{\infty} j a_j U_{j-1}(u)\ge 0 \quad \forall u\in[-1,1] \end{array}. \qquad (14)$$

<u>Example 1A</u>: A case of particular importance is that of the dithering sequence $\{\mathbf{u}_k\}$ with *uniformly* distributed IID random variables, i.e. $G'(u)=1/2$ in $[-1,1]$ and therefore $G(u)=(u+1)/2$. Since $T_1(u)=u$ this leads by inspection to $a_0=0$, $a_1=1$ and $a_k=0$ for $k=2,3,4,\ldots$.

<u>Example 1B</u>: The undithered case of Figure 1 can be thought of as the *limiting case* of $\mathbf{u}_k\equiv 0$ which has CDF $G(u)=0$ for $u\in[-1,0)$ and $G(u)=1$ for $u\in(0,1]$. Although G is discontinuous at $u=0$ its series expansion is valid for $u\ne 0$ implying $a_{2k}=0$ and $a_{2k+1}=\dfrac{4(-1)^k}{(2k+1)\pi}$ for $k=0,1,2,\ldots$

<u>Example 1C</u>: Let $a_1,a_3\ne 0$ and all other coefficients a_k be zero. Since $T_1(u)=u$ and $T_3(u)=4u^3-3u$ we have $G(u)=\frac{1}{2}+\frac{a_1}{2}u+\frac{a_3}{2}(4u^3-3u)$. For G to be a CDF Eqs. (14) imply $a_1+a_3=1$ and $2G'(u)=a_1+a_3(12u^2-3)\ge 0$ for every $u\in[-1,1]$. Since $2G'(u)$ achieves its minimum either at $u=0$ or at $u=1$, depending on the sign of a_3, it is $G'(u)\ge 0$ for every $u\in[-1,1]$ if and only if $a_1-3a_3\ge 0$ and $a_1+9a_3\ge 0$. Combining the above, G is a CDF if and only if $a_1+a_3=1$, $a_1+9a_3\ge 0$ and $a_1-3a_3\ge 0$. The (solution) feasible set of a_1,a_3 is $a_1=(6+3\rho)/8$ and $a_3=(2-3\rho)/8$ with $\rho\in[0,1]$ shown in thick line in Fig. 5.

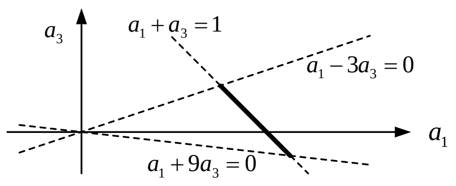

Figure 5: Feasible set of a_1,a_3 in Example 1C (thick line)

<u>Example 1D</u>: Let $a_1,a_5\ne 0$ and all other coefficients a_k be zero. It is $G(u)=\frac{1}{2}+\frac{a_1}{2}T_1(u)+\frac{a_5}{2}T_5(u)$ where $T_1(u)=u$ and $T_5(u)=16u^5-20u^3+5u$. Eqs. (14) imply $a_1+a_5=1$ and $2G'(u)=a_1+a_5P(u)\ge 0$ for every $u\in[-1,1]$ where we have set $P(u)=80u^4-60u^2+5$. The maximum and minimum values of $P(u)$ in $[-1,1]$ are 25 and $-25/4$ respectively and so $G'(u)\ge 0$ for every $u\in[-1,1]$ if and only if $a_1+25a_5\ge 0$ and $4a_1-25a_5\ge 0$. Combining the above we conclude that G is a CDF if and only if $a_1+a_5=1$, $a_1+25a_5\ge 0$ and $4a_1-25a_5\ge 0$. The feasible set of a_1,a_5 is given by $a_1=\frac{25}{24}(1-\rho)+\frac{25}{29}\rho$, $\quad a_5=-\frac{1}{24}(1-\rho)+\frac{4}{29}\rho$, $\quad \rho\in[0,1]$ with a graph very similar to that in Fig. 5.

<u>Example 1E</u>: Let $a_1,a_3,a_5\ne 0$ and all other coefficients a_k be zero. It is $G(u)=\frac{1}{2}+\frac{a_1}{2}T_1(u)+\frac{a_3}{2}T_3(u)+\frac{a_5}{2}T_5(u)$ and relationships (14) become $a_1+a_3+a_5=1$ and $2G'(u)=80a_5u^4+(12a_3-60a_5)u^2+a_1-3a_3+5a_5\ge 0$ for every $u\in[-1,1]$. It turns out that the feasible set of a_3, a_5, with a_1 derived from $a_1+a_3+a_5=1$, is shown in Fig. 6 below.

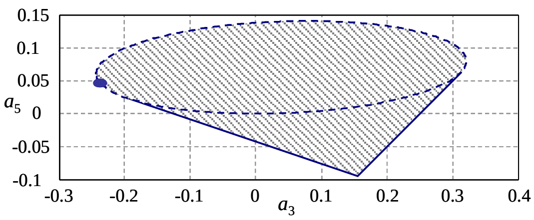

Figure 6: Feasible set of a_3,a_5 in Example 1E shown in gray. Coefficient a_1 is derived from $a_1+a_3+a_5=1$.

The following Lemma whose proof is available in the Appendix expresses the average autocorrelation of $\{\mathbf{x}_k\}$ as a function of the coefficients a_j, $j=0,1,2,\ldots$.

<u>Lemma 2</u>: *Consider the Chebyshev series expansion in Eq.* (11) *of the CDF G of the IID random sequence $\{\mathbf{u}_k\}$. The average autocorrelation of the random sequence $\{\mathbf{x}_k\}$ is given by* (15) *where δ_k is the discrete-time Dirac function.*

$$\overline{r}_x(k)=a_0^{\,2}+\frac{1}{2}\sum_{j=1}^{\infty}a_j^{\,2}\cos(j\Omega k)+\left(1-a_0^{\,2}-\frac{1}{2}\sum_{j=1}^{\infty}a_j^{\,2}\right)\delta_k \qquad (15)$$

According to Eq. (15), $\overline{r}_x$ is composed of a DC term, an impulse term at $k=0$ and harmonics of $\cos(\Omega k)$. It is remarkable that the amplitude of the j^{th} harmonic is $a_j^{\,2}/2$, i.e. proportional to the square of the projection of CDF G to the j^{th} Chebyshev polynomial according to Eqs. (12). Therefore, by selecting CDF G appropriately we can "shape" the average autocorrelation $\overline{r}_x$. Note that since time is discrete here, all frequency components in Eq. (15) with $j\ge\Omega/\pi$

suffer from aliasing and fold into the frequency interval $\omega \in [0, 2\pi)$. Specifically, since the DTFT of $\cos(j\Omega k)$ is [47] $\pi \sum_{m=-\infty}^{\infty} \left(\delta(\omega - j\Omega - 2\pi m) + \delta(\omega + j\Omega - 2\pi m) \right)$ the frequency contributions of $\cos(j\Omega k)$ are at $(\omega - j\Omega) \bmod 2\pi$ and $(\omega + j\Omega) \bmod 2\pi$. Some of the harmonics may fold very close to the carrier frequency Ω. The detailed spectrum of $\overline{r}_x$ is given by Lemma 3 whose proof is in the appendix.

<u>Lemma 3</u>: *The DTFT* $s_x(\omega)$ *of the average autocorrelation function* $\overline{r}_x$ *can be expressed as*

$$s_x(2\pi f T_S) = \frac{1}{T_S} \left(S_H(f) + S_N(f) + S_0(f) \right) \tag{16}$$

where the three components $S_H(f)$, $S_N(f)$ *and* $S_0(f)$ *are*

$$S_H(f) = \sum_{j=1}^{\infty} \frac{a_j^2}{4} \sum_{k=-\infty}^{\infty} \left(\delta\left(f - \frac{k}{T_S} - \frac{j\Omega}{2\pi T_S} \right) + \delta\left(f - \frac{k}{T_S} + \frac{j\Omega}{2\pi T_S} \right) \right) \tag{17}$$

$$S_N(f) = T_S \left(1 - a_0^2 - \frac{1}{2} \sum_{j=1}^{\infty} a_j^2 \right) \tag{18}$$

and

$$S_0(f) = a_0^2 \cdot \sum_{k=-\infty}^{\infty} \delta\left(f - \frac{k}{T_S} \right) \tag{19}$$

Combining Lemmas 1 and 3 we derive the PSD of the stochastic process $\mathbf{x}(t)$ parameterized on the coefficients a_j of the Chebyshev polynomial series of CDF G in Eq. (11).

<u>Corollary 1</u>: *The PSD of the stochastic process* $\mathbf{x}(t)$ *is*

$$S_x(f) = \text{sinc}^2(f T_S) \cdot \left(S_H(f) + S_N(f) + S_0(f) \right) \tag{20}$$

where the three components $S_H(f)$, $S_N(f)$ *and* $S_0(f)$ *are given by Eqs.* (17), (18) *and* (19) *respectively.* □

<u>Remark 2</u>: A) Since $s_x(\omega)$ with $\omega = 2\pi f T_S$ is the result of DTFT, it is periodic on f with period $f_s = 1/T_S$. Such are all three components $S_H(f)$, $S_N(f)$ and $S_0(f)$ as well.

B) Note that the PSD component $S_H(f)$ captures the desirable signal at frequency $\Omega/(2\pi T_S)$ as well as the intermodulation products at frequencies $k/T_S \pm j\Omega/(2\pi T_S)$, $j = 1, 2, 3, ...$ and $k \in \mathbb{Z}$.

C) PSD component $S_N(f)$ is independent of the frequency and captures the noise floor level (in the continuous-time spectrum) introduced by the dithering.

D) If[5] $\Omega = 2\pi w/q$, then $S_H(f)$ may partially include the DC component whose other part is captured by $S_0(f)$ along with harmonics of the sampling frequency.

E) $S_x(f)$ has no power at the fundamental and harmonics of the sampling frequency $f_S = 1/T_S$ because the factor $\text{sinc}^2(f T_S)$, corresponding to the ZOH stage in the quantization scheme in Fig. 4, is zero for all $f = k/T_S$, $k \neq 0$. So we can ignore the terms $\delta(f - k/T_S)$ with $k \neq 0$.

If $\Omega = 2\pi w/q$ then the frequency components of $S_H(f)$ appear at $(k \pm jw/q)/T_S = (qk \pm jw)/(qT_S)$ for $j = 1, 2, 3, ...$ and $k \in \mathbb{Z}$ which are positive and negative harmonics of the fundamental frequency $1/(qT_S)$. Based on this and after some algebraic manipulation of Eq. (20) we get Theorem 1 which provides explicitly the power of each harmonic at $h/(qT_S)$, $h \in \mathbb{Z}$. The proof of Theorem 1 is available in the Appendix.

<u>Theorem 1</u>: *For angular frequency* $\Omega = 2\pi w/q$ *with* $0 < w < q/2$ *and* $\gcd(w, q) = 1$ *we have that*

$$S_x(f) = \text{sinc}^2(f T_S) \cdot \left(\tilde{S}_H(f) + S_N(f) + \tilde{S}_0(f) \right) \tag{21}$$

where $S_N(f)$ *is as in Lemma 3 and* $\tilde{S}_H(f)$ *and* $\tilde{S}_0(f)$ *are*

$$\tilde{S}_H(f) = \frac{1}{4} \sum_{h=1}^{\infty} b_h \left(\delta\left(f - \frac{h}{qT_S} \right) + \delta\left(f + \frac{h}{qT_S} \right) \right) \tag{22}$$

and

$$\tilde{S}_0(f) = \frac{3a_0^2}{4} \sum_{k=1}^{\infty} \left(\delta\left(f - \frac{k}{T_S} \right) + \delta\left(f + \frac{k}{T_S} \right) \right) + \frac{b_0 + 3a_0^2}{4} \delta(f) \tag{23}$$

respectively. Here, for $h = 0, 1, 2, ...$ *we have defined*[6]

$$b_h \triangleq \sum_{r=-\infty}^{\infty} a_{I(h,r)}^2 \tag{24}$$

where $I(h, r) = |j_1 h + qr|$ and the integer pair[7] (j_1, k_1) *is* a (any) solution of the *Diophantine equation* $wj_1 + qk_1 = 1$. *In particular, coefficient* b_w *of the frequency component at* $\pm\Omega/(2\pi T_S) = \pm w/(qT_S)$ *is* $b_w = \sum_{r=-\infty}^{\infty} a_{|1+qr|}^2$. *Finally, it is*

$$S_H(f) + S_0(f) = \tilde{S}_H(f) + \tilde{S}_0(f) \tag{25}$$

where $S_H(f)$ *and* $S_0(f)$ *are defined in Eqs.* (17) and (19).□

Both expressions $S_H(f)$ and $\tilde{S}_H(f)$ capture the desirable signal and the intermodulation products, they differ only in the DC and harmonic components $f = k/T_S$, $k \neq 0$. However, $S_H(f)$ sums with respect to coefficients a_j, $j = 1, 2, 3, ...$ (first) each of which contributes to the amplitude of *many* frequency components. So $S_H(f)$ relates directly with the Chebyshev expansion of the CDF G of the dithering sequence. On the other hand $\tilde{S}_H(f)$ provides the amplitude

[5] That is, if $\Omega/(2\pi)$ is a rational number.

[6] *b_h is the amplitude of the frequency component at $\pm h/(qT_S)$ for $h = 1, 2, ...$ and b_0 is part of the DC component.*

[7] *k_1 is not involved in the expressions of Theorem 1.*

of each frequency component, b_h, $h=1,2,3,\ldots$ as a sum of squares of infinitely many a_j s.

Remark 3: To derive coefficient b_h, $h=0,1,2,\ldots$ we first have to find a solution (j_1,k_1) of the Diophantine equation $wj_1+qk_1=1$ using the Euclidean algorithm (e.g. the "gcd" function in MATLAB). Since by assumption $\gcd(w,q)=1$ this is always possible and any other solution of the equation is of the form

$$\left(j_1',k_1'\right)=\left(j_1,k_1\right)+\rho\left(q,-w\right) \tag{26}$$

for some $\rho\in\mathbb{Z}$. Then $b_h \triangleq \sum_{r=-\infty}^{\infty} a^2_{|j_1h+qr|}$ where only j_1 is used in the index $|j_1h+qr|$. Moreover note that the sum is over $r\in\mathbb{Z}$ and so according to Eq. (26) it does not depend on the particular choice of the solution of the Diophantine equation, i.e. replacing j_1 by j_1' would only shift $r\in\mathbb{Z}$ by $h\rho$.

Remark 4: From Eq. (24) we conclude that the contributions of coefficients a_j, $j=0,1,2,\ldots$ to the power of frequency component at $h/(qT_S)$ in Eq. (22) are cumulative since $a^2_{I(h,r)}\geq 0$. Therefore the smaller the set of nonzero coefficients a_j is, the smaller the set of frequency components present in $\tilde{S}_H(f)$ will be. The same is true for $S_x(f)$ and so for $\tilde{S}_0(f)$ as well since a_j s also act cumulatively in Eq. (23).

Example 2A: Following Example 1A with $a_0=0$, $a_1=1$ and $a_k=0$ for $k=2,3,4,\ldots$, Lemma 3 implies that $S_0(f)=0$, $S_N(f)=T_S/2$ and most importantly,

$$S_H(f)=\frac{1}{4}\sum_{k=-\infty}^{\infty}\left(\delta\left(f-\frac{k}{T_S}-\frac{\Omega}{2\pi T_S}\right)+\delta\left(f-\frac{k}{T_S}+\frac{\Omega}{2\pi T_S}\right)\right).$$

If $\Omega=2\pi w/q$ the frequency components of $S_H(f)$ are at $\frac{k}{T_S}\pm\frac{\Omega}{2\pi T_S}=\frac{kq\pm w}{q}f_S$, $k\in\mathbb{Z}$. So the only two frequency components in the interval $(0,f_S)$ are at $(w/q)f_S$ and $(1-w/q)f_S$, and have the same power. Also, the spectrum in any interval $(rf_S,(r+1)f_S)$, $r\in\mathbb{Z}$ is a replica of the spectrum in $(0,f_S)$ according to Remark 2. For $w=25$ and $q=64$ the PSD of the simulated random sequence $\mathbf{x}_k=\operatorname{sgn}(\cos(\Omega k)-\mathbf{u}_k)$, $k\in\mathbb{Z}$ is shown in Fig. 7. It agrees completely with $S_H(f)$. Finally, the PSD $S_x(f)$ of $\mathbf{x}(t)$ is that of Fig. 7 weighted by the factor $\operatorname{sinc}^2(fT_S)$ according to Eq. (10).

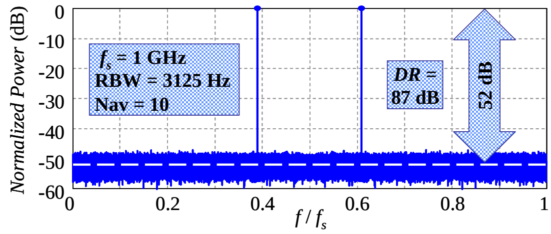

Figure 7: PSD of simulated random sequence $\{\mathbf{x}_k\}$ when $a_0=0$, $a_1=1$ and $a_k=0$, $k=2,3,4,\ldots$; $w=25$ and $q=64$; $f_S=1\,GHz$, Resolution BW = 3125 Hz and waveform averaging Nav=10 runs.

Example 2B: The PSD $s_x(2\pi fT_S)$ corresponding to Example 1B is shown in Fig. 2.

Example 2C: Following Example 1C with $\rho=1$ we get that $a_1=9/8$, $a_3=-1/8$ and all other coefficients a_k are zero. For $w=25$ and $q=64$ the PSD of the simulated random sequence $\mathbf{x}_k=\operatorname{sgn}(\cos(\Omega k)-\mathbf{u}_k)$, $k\in\mathbb{Z}$ is shown in Fig. 8. From Eqs. (17), (18) and (19) we derive directly that the only frequency components present are at frequencies $\frac{k}{T_S}\pm\frac{\Omega}{2\pi T_S}=\left(k\pm\frac{25}{64}\right)f_S$ and $\frac{k}{T_S}\pm\frac{3\Omega}{2\pi T_S}=\left(k\pm\frac{75}{64}\right)f_S$ with $k\in\mathbb{Z}$. So the only frequencies in the spectrum $(0,f_S)$ are at $(0+25/64)f_S$ and $(1-25/64)f_S$ from the first expression, corresponding to the fundamental and its image; and, $(-1+3\cdot 25/64)f_S$ and $(2-3\cdot 25/64)f_S$ from the second one, corresponding to the 3rd harmonic and its image. Alternatively one can identify the frequency components within $(0,f_S)$ from Eq. (24) of Theorem 1 via the following steps: find a solution of the Diophantine equation $25j_1+64k_1=1$, e.g. $(j_1,k_1)=(-23,9)$ and use it to solve Diophantine equations $I(h,r)=|-23h+64r|=1$ and $I(h,r)=|-23h+64r|=3$ for $h=0,1,2,\ldots,63$ and $r\in\mathbb{Z}$ (since a_1 and a_3 are the only nonzero coefficients). We derive that for $h=0,1,2,\ldots,63$ the only nonzero b_h's are $b_{11}=(1/8)^2$, $b_{25}=(9/8)^2$, $b_{39}=(9/8)^2$ and $b_{53}=(1/8)^2$, corresponding to frequencies $(11/64)f_S$, $(25/64)f_S$, $(39/64)f_S$ and $(53/64)f_S$ respectively. The result agrees with the simulation in Fig. 8.

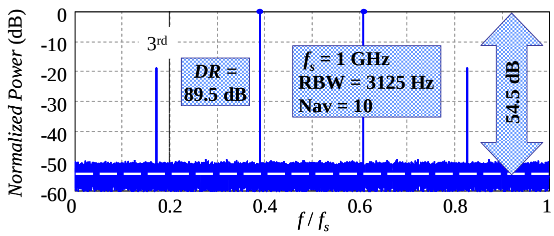

Figure 8: PSD of simulated random sequence $\{\mathbf{x}_k\}$ when $a_1=9/8$, $a_3=-1/8$ and all other coefficients $a_k=0$; $w=25$ and $q=64$; and with the same remaining parameters as in Fig. 7.

Example 2D: Fig. 9 shows the PSD of the simulated random sequence $\mathbf{x}_k = \operatorname{sgn}(\cos(\Omega k) - \mathbf{u}_k)$, $k \in \mathbb{Z}$ when $a_1 = 25/24$, $a_5 = -1/24$ and all other coefficients $a_k = 0$, i.e., following Example 1D with $\rho = 0$, $w = 25$ and $q = 64$. The derivation of the frequencies of the components in $(0, f_S)$ is similar to that in Example 2C. From Theorem 1 we derive that for $h = 0,1,2,\ldots,63$ it is $b_3 = (1/24)^2$, $b_{25} = (25/24)^2$, $b_{39} = (25/24)^2$ and $b_{61} = (1/24)^2$, corresponding to frequencies $(3/64) f_S$, $(25/64) f_S$, $(39/64) f_S$ and $(61/64) f_S$ respectively; and all other b_h are zero. This agrees with the simulation in Fig. 9.

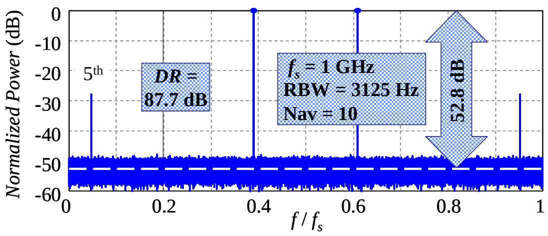

Figure 9: PSD of simulated random sequence $\{\mathbf{x}_k\}$ when $a_1 = 25/24$, $a_5 = -1/24$ and all other coefficients $a_k = 0$; $w = 25$ and $q = 64$; and with the same remaining parameters as in Fig. 7.

Example 2E: Fig. 10 shows the PSD of the simulated random sequence $\mathbf{x}_k = \operatorname{sgn}(\cos(\Omega k) - \mathbf{u}_k)$, $k \in \mathbb{Z}$ when $a_1 = 1.1906$, $a_3 = -0.2375$, $a_5 = 0.0469$ and all other coefficients a_k are zero. It follows Example 1E with (a_3, a_5) corresponding to the big dot on the ellipse in Fig. 6. The derivation of the frequencies of the components in $(0, f_S)$ is similar to that in Example 2C. The 3rd and the 5th harmonics (and only those) are present in the spectrum as expected. From Theorem 1 we derive that for $h = 0,1,2,\ldots,63$ it is $b_3 = 0.0022$, $b_{11} = 0.0564$, $b_{25} = 1.4175$, $b_{39} = 1.4175$, $b_{53} = 0.0564$ and $b_{61} = 0.0022$, corresponding to frequencies 3, 11, 25, 39, 53 and 61 $\times f_S/64$ respectively; and all other b_h are zero. This agrees with the simulation in Fig. 10.

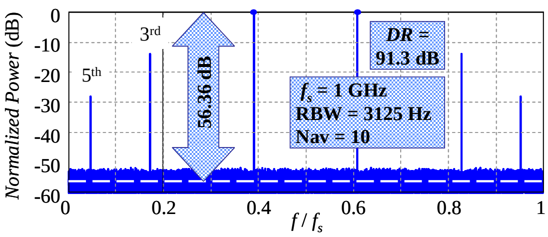

Figure 10: PSD of simulated random sequence $\{\mathbf{x}_k\}$ when $a_1 = 1.1906$, $a_3 = -0.2375$, $a_5 = 0.0469$ and all other coefficients $a_k = 0$; $w = 25$ and $q = 64$; same parameters as in Fig. 7.

Finally, coefficients b_h, $h = 0,1,2,\ldots$ have periodicity and mirroring properties inherited by those of the PSD $\tilde{S}_H(f)$ and $\tilde{S}_0(f)$ (see also Remark 2A) which are stated below. The proof of the Lemma is in the Appendix.

Lemma 4: For every $h = 0,1,2,\ldots$ and $k, \ell \in \mathbb{Z}$ such that $kq + h \geq 0$ and $\ell q - h \geq 0$ it is $b_{kq+h} = b_{\ell q - h} = b_h$. In particular we have that $b_h = b_{h \bmod q} = b_{q-(h \bmod q)}$ for every $h = 0,1,2,\ldots$. □

V. Spurs-Free Spectrum, Dynamic Range and the Trade-Off Between Noise Floor and Harmonics

In most practical cases the desirable frequency component is the one at $\Omega/(2\pi T_S) = (w/q) f_S$. Example 2A illustrated that if $a_0 = 0$, $a_1 = 1$ and $a_k = 0$ for $k = 2,3,4,\ldots$ then the only two components in the frequency interval $(0, f_S)$ are at $(w/q) f_S$ and $(1 - w/q) f_S$. This spurs-free output[8] however comes at the cost of noise floor level $S_N(f) = T_S/2$. A natural question is whether a different choice of coefficients a_j could lead to lower noise floor, or, whether the noise floor can be reduced by allowing some of the harmonics to be present in the spectrum.

This Section provides necessary and sufficient conditions for coefficients a_j, for achieving spurs-free output, i.e. for having only the frequency components at $(w/q) f_S$ and $(1 - w/q) f_S$ in the interval $(0, f_S)$. These can potentially lead to values of coefficients a_j resulting in lower noise floor level $S_N(f)$ than that with $a_0 = 0$, $a_1 = 1$ and $a_k = 0$ for $k = 2,3,4,\ldots$ The Section also illustrates how we can trade off spectral clarity (i.e. allowing some harmonics to be present) for reducing the noise floor level.

Note that the weighting factor $\operatorname{sinc}^2(f T_S)$ in Eq. (21) eliminates all components at frequencies $k f_S$, $k \in \mathbb{Z} - \{0\}$, i.e. all clock harmonics except the DC, and only these. This indicates the qualitative difference between the PSDs $S_x(f)$, $\tilde{S}_H(f)$ and how these two can be used indistinguishably in the following Lemmas and Theorem.

We have the following Lemma whose proof results directly from Lemma 4 and is omitted.

Lemma 5: Following the assumptions of Theorem 1; if the frequency component at $\Omega/(2\pi T_S) = w/(q T_S)$ is present in $S_x(f)$, i.e. if $b_w > 0$, then all frequency components at

$$\frac{k}{T_S} \pm \frac{\Omega}{2\pi T_S} = \left(k \pm \frac{w}{q}\right) f_S, \qquad k \in \mathbb{Z} \tag{27}$$

are present as well, i.e., $b_{qk+w} > 0$ and $b_{qk-w} > 0$, $k = 1,2,3,\ldots$ □

Consider Lemma 5 in conjunction with Lemma 4. The last one also implies that if a component at a frequency beyond

[8] Note that the image frequency component at $(1 - w/q) f_S$ has to be there because of the discrete-time nature of the quantized sinewave.

those in Eq. (27) is present $S_x(f)$, then, because of the spectral periodicity and mirroring, a corresponding frequency component is present within $(0, f_S/2)$.

We cannot avoid having all frequencies in Eq. (27) present when the desirable frequency component at $w/(qT_S)$ is generated. Yet we can determine the *maximal* set of nonzero coefficients a_j generating *only* frequencies $w/(qT_S)$ and those in Eq. (27). Note that the maximal set does exist because of Remark 4. Lemma 6 provides the answer.

Lemma 6: Assume that $\Omega = 2\pi w/q$ with $0 < w < q/2$ and $\gcd(w,q) = 1$, and let $\mathbf{J} \triangleq \{0,1,rq,rq \pm 1 \mid r = 1,2,3,...\}$ and $\mathbf{H} \triangleq \{0,w,rq,rq \pm w \mid r = 1,2,3,...\}$ be two sets of nonnegative integers. Then $a_j = 0$ for every $j \in \{0,1,2,...\} - \mathbf{J}$ if and only if $b_h = 0$ for every $h \in \{0,1,2,...\} - \mathbf{H}$. □

The proof of Lemma 6 is available in the Appendix. Lemma 7 below provides a similar and partially complementary result based directly on expression $b_w = \sum_{r=-\infty}^{\infty} a_{|1+qr|}^2$ of Theorem 1. Its proof is by observation and is omitted.

Lemma 7: Under the assumptions of Lemma 6, the frequency component at $\Omega/(2\pi T_S) = (w/q) f_S$ is present[9], i.e., $b_w > 0$ if and only if there exists some $j \in \{1, rq \pm 1 \mid r = 1,2,3,..\}$ such that $a_j \neq 0$. □

The following Theorem states conditions for spurs-free output within the frequency interval $(0, f_S/2)$. It results from combining Lemma 6 and Lemma 7 and its proof is omitted.

Theorem 2: [Spurs-Free Output]: Under the assumptions of Lemma 6 there is only one frequency component present[9] in $(0, f_S/2)$, which is at frequency $(w/q) f_S$, if and only if $a_j = 0$ for every $j \in \{0,1,2,...\} - \mathbf{J}$ and there exists some $j \in \{1, rq \pm 1 \mid r = 1,2,3,..\}$ such that $a_j \neq 0$. □

The result of Theorem 2 extends to frequency interval $(0, f_S)$ where both $(w/q) f_S$ and $(1 - w/q) f_S$ frequency components are present, as well as to the periodic replicas of the spectrum (see Remark 2) of $\tilde{S}_H(f)$, and to those of $S_x(f)$ taking into account the weighting factor $\mathrm{sinc}^2(f T_S)$.

Remark 5: According to Theorem 2, the case of $a_0 = 0$, $a_1 = 1$ and $a_k = 0$ for $k = 2,3,4,...$ is probably the simplest one guarantying spur-less output *for every pair of integers* w,q satisfying $0 < w < q/2$ and $\gcd(w,q) = 1$.

Example 2A illustrates the case of $a_0 = 0$, $a_1 = 1$ and $a_k = 0$ for $k = 2,3,4,...$ which according to Theorem 2 implies a spurs free spectrum, shown in Fig. 7. Also Fig. 11 below captures a part of a realization of the random sequence $\{\mathbf{x}_k\}$ generated in Example 2A along with undithered sequence $\mathrm{sgn}(\cos(2\pi kw/q))$ and the corresponding continues-time sinewave. Since $w/q = 25/64 \cong 0.39$ is close to 1/2 (Nyquist frequency) both discrete-time waveforms tend to change sign almost at every clock. However, they tend to differ from each other when the sampling of the cosine occurs near its zero crossings.

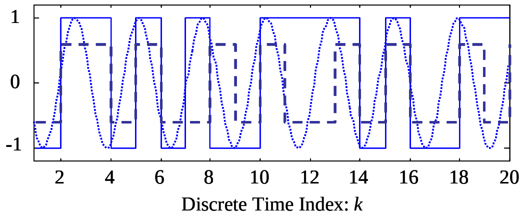

Figure 11: Time-Domain signals related to Example 2A. Sequence x_k is the solid ± 1 waveform. $\mathrm{sgn}(\cos(2\pi kw/q))$ is the dashed waveform scaled to 60%. The corresponding continuous-time sinewave $\cos(2\pi tw/(qT_S))$ is shown in dotted line.

Example 3: More examples of PSD of the simulated random sequence $\mathbf{x}_k = \mathrm{sgn}(\cos(\Omega k) - \mathbf{u}_k)$, $k \in \mathbb{Z}$ when $a_0 = 0$, $a_1 = 1$ and $a_k = 0$ for $k = 2,3,4,...$ are shown in Figs. 12, 13 and 14 for a variety of values of w, q, f_s and waveform averaging runs Nav. In Fig. 14, the PSD for different values of w (arbitrarily chosen) are graphically overlapped. As expected from Theorem 2, all PSD are spurs-free.

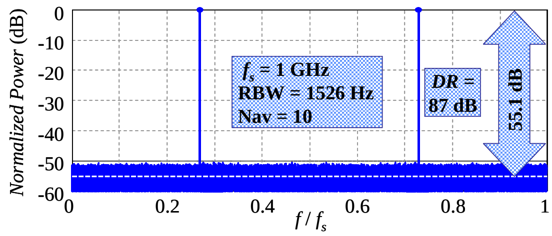

Figure 12: PSD of simulated random sequence $\{\mathbf{x}_k\}$ when $a_0 = 0$, $a_1 = 1$ and $a_k = 0$, $k = 2,3,4,...$; $w = 17723$, $q = 2^{16}$; $f_S = 1\,GHz$, Resolution BW = 1526 Hz and waveform averaging Nav=10 runs.

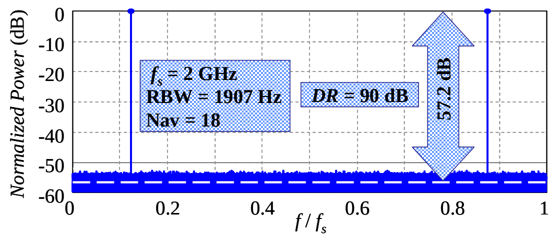

Figure 13: PSD of simulated random sequence $\{\mathbf{x}_k\}$ when $a_0 = 0$, $a_1 = 1$ and $a_k = 0$, $k = 2,3,4,...$; $w = 2^{16} - 1$, $q = 2^{19}$; $f_S = 2\,GHz$, Resolution BW = 1907 Hz and waveform averaging Nav=18 runs.

[9] One can consider PSD $S_x(f)$ or $\tilde{S}_H(f)$.

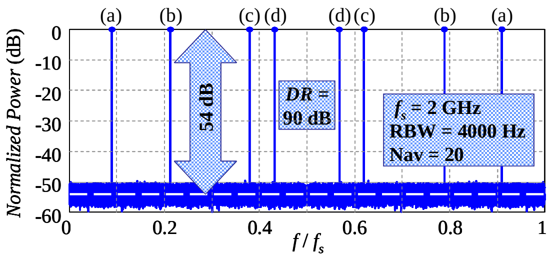

Figure 14: PSD of simulated random sequence $\{\mathbf{x}_k\}$ when $a_0 = 0$, $a_1 = 1$ and $a_k = 0$, $k = 2,3,4,...$; w = 9023(a), 21241(b), 37981(c) and 43197(d), and $q = 10^5$; $f_S = 2\,GHz$, Resolution BW = 4 kHz and waveform averaging Nav=20 runs.

Example 4: Another case of PSD of the simulated random sequence $\{\mathbf{x}_k\}$ when $a_0 = 0$, $a_1 = 1$ and $a_k = 0$, $k = 2,3,4,...$ is shown in Fig. 15. It corresponds to the PSD in Fig. 3 of the undithered quantized sinewave.

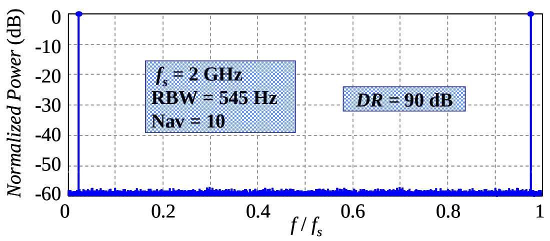

Figure 15: PSD of simulated random sequence $\{\mathbf{x}_k\}$ when $a_0 = 0$, $a_1 = 1$ and $a_k = 0$, $k = 2,3,4,...$; $w = 5831$, $q = 2^{18}$; $f_S = 2\,GHz$, Resolution BW = 545 Hz and waveform averaging Nav=10 runs.

The corresponding time-domain waveforms of this example are shown in Fig. 16 below. Since $w/q = 5831/2^{18} \cong 0.022$ is very small the dithered waveform (sequence x_k) resembles Pulse Width Modulation with some randomness.

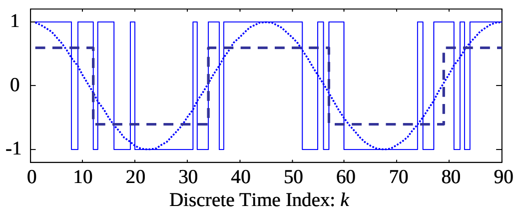

Figure 16: Time-Domain signals related to Example 4. Sequence x_k is the solid ± 1 waveform. $\text{sgn}(\cos(2\pi k w/q))$ is the dashed waveform scaled to 60%. The corresponding continuous-time sinewave $\cos(2\pi t w/(q T_s))$ is shown in dotted line.

A. Noise Floor & Dynamic Range

Consider the frequency components in $\tilde{S}_H$ and the noise floor captured by S_N in Eq. (21). We define the Dynamic Range (DR) of the output as the ratio of the power $b_w/4$ of the desirable frequency component at $\Omega/(2\pi T_S) = (w/q)\,f_S$ over the noise power spectral density at the same frequency, i.e., $S_N((w/q)\,f_S)$, which equals $T_S\left(1 - a_0^2 - \left(\sum_{j=1}^{\infty} a_j^2\right)/2\right)$.

Replacing the value of b_w from Theorem 1 and expressing DR in logarithmic scale we have (in dB):

$$DR = 10\log_{10}\left(\frac{\sum_{r=-\infty}^{\infty} a_{|1+qr|}^2}{1 - a_0^2 - \frac{1}{2}\sum_{j=1}^{\infty} a_j^2}\right) + 10\log_{10}(f_S) - 6.02 \quad (28)$$

The definition of DR applies directly to the total output spectrum $S_x(f)$ using Eq. (28) as well because the factor $\text{sinc}^2(f T_S)$ in Eq. (21) multiplies both $\tilde{S}_H$ and S_N. Also, note that the summand $10\log_{10}(f_S)$ is expected since the power of the sinewave's quantization error is spread in frequency bandwidth proportional to the sampling frequency. Finally, the DR can be defined similarly in the case that a different frequency component is the desirable one.

Example 5A: In the case of $a_0 = 0$, $a_1 = 1$ and $a_k = 0$ for $k = 2,3,4,...$, i.e., when the probability density function of the dither is *uniform*, we have from Eq. (28) that the DR is $DR = 10\log_{10}(f_S) - 3.01$ dB. In the case of Example 2A where the PSD is shown in Fig. 7, the dashed white line indicates the averaged noise floor level. For $f_S = 1\,GHz$ we get $DR \cong 87$ dB. Subtracting $10\log_{10}(RBW)$ dB, where $RBW = 3125\,Hz$, to account for the resolution BW used for the simulation in Fig. 7, we get a very good match to the simulated 52 dB (Fig. 7).

Example 5B: The undithered case in Fig. 2 has $DR = \infty$ since there is no noise floor although the spectrum is full of strong spurious frequency components.

Example 5C: We follow Example 1C with $a_1 = (6+3\rho)/8$, $a_3 = (2-3\rho)/8$ and $\rho \in [0,1]$, and all other a_k equal zero. Assuming that $q > 4$ implies $\sum_{r=-\infty}^{\infty} a_{|1+qr|}^2 = a_1^2$ and Eq. (28) gives $DR = 10\log_{10}\left(\frac{2a_1^2}{2-(a_1^2+a_3^2)}\right) + 10\log_{10}(f_S) - 6.02$ dB. Using the expressions of a_1 and a_3 above, DR becomes a function of ρ, strictly increasing, and with maximum value $DR = 10\log_{10}(f_S) - 0.55$ (dB) for $\rho = 1$, corresponding to $a_1 = 9/8$ and $a_3 = -1/8$. DR here is about 2.5 dB higher than in Example 5A but the 3rd harmonic is present here as it is shown in Fig. 8.

Example 5D: Following Example 1D we assume that $a_1 = \frac{25}{24}(1-\rho) + \frac{25}{29}\rho$, $a_5 = -\frac{1}{24}(1-\rho) + \frac{4}{29}\rho$ and $\rho \in [0,1]$ and all other a_k are zero. Again, it is convenient to assume further that $q > 6$ implying $\sum_{r=-\infty}^{\infty} a_{|1+qr|}^2 = a_1^2$ which via Eq. (28)

gives $DR = 10\log_{10}\left(\dfrac{2a_1^2}{2-\left(a_1^2+a_5^2\right)}\right)+10\log_{10}\left(f_S\right)-6.02$ dB. Replacing the expressions of a_1 and a_5 in DR, the last one becomes a function of ρ, strictly decreasing with maximum value $DR = 10\log_{10}\left(f_S\right)$-2.25 dB for $\rho = 0$, corresponding to $a_1 = 25/24$ and $a_5 = -1/24$. DR here is only about 0.75 dB higher than in Example 5A and the 5th harmonic is present here as it is shown in Fig. 9.

Example 5E: The values of a_1, a_3 and a_5 given in Example 2E are the ones maximizing DR when all other coefficients a_k, $k \neq 1,3,5$ are zero; the pair (a_3, a_5) corresponds to the big dot on the ellipse in Fig. 6. In this case it is $DR = 10\log_{10}\left(f_S\right)+1.31$ (dB), which is about 4.3 dB higher than using uniformly distributed dither as in Example 5A.

Example 6: Differentiating the CDF G we derive the probability density function G' which is shown in Fig. 17 below for each of the cases in Examples 5A, C, D and E. The function G' is a polynomial of zero, second, fourth and fourth order respectively with nonnegative values in $[-1,1]$.

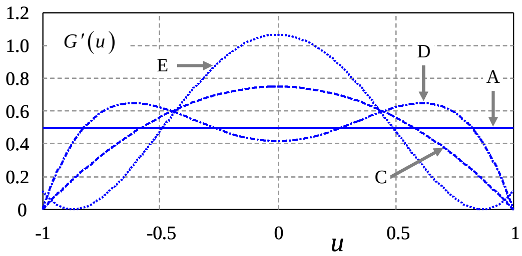

Figure 17: Probability density functions of Examples 5A,C,D and E.

Examples 5C, D and E, where the 3rd harmonic, the 5th harmonic, and both of them, are present, respectively, demonstrate higher DR relatively to uniformly distributed dither in Example 5A. In some sense, the dithering spreads the harmonics' power over the sampling bandwidth converting their line spectral power into continuous noise floor. Keeping some of the harmonics present in the spectrum means less power is converted to noise.

One can also compare all four Examples 5A, C, D and E with the (extreme) undithered case of Example 5B which has infinite DR (no noise floor) but also countably infinite and powerful discrete spurious tones (harmonics).

The above comparisons demonstrate the possibility to shape the CDF so that the DR is improved (compared to uniform dithering) by allowing a number (or all) of the harmonics, located in unconcerned frequency intervals, to be present without harming the quality of the generated signal.

VI. Conclusions

Single-Bit Nyquist-rate quantization of sinewave with random dithering using sequences of independent and identically distributed random variables has been analyzed mathematically.

The spectrum of the output stochastic process has been derived analytically as a function of the coefficients of the Chebyshev polynomials series expansion of the dither's Cumulative Distribution Function (CDF).

The frequencies and the powers of the frequency components have been derived explicitly. Necessary and sufficient conditions for spurs-free output have been derived and related to the dither's CDF. In particular, uniformly distributed dither with range equal to that of the sinewave results in a spectrum identical to that of sampled sinewave (of infinite amplitude resolution) with an additive noise floor.

The noise floor level due to random dithering has been derived analytically and the output dynamic range has been defined and calculated explicitly for certain classes of the dither's CDF.

The trade-off between selected frequency-spurs presense and dynamic range improvement has been studied and dynamic range optimization has been established for certain classes of the dither's CDF. An improvement of about 4.3 dB has been found when the third and fifth harmonics are allowed to be present.

A number of examples based on MATLAB simulation have been discussed illustrating the presented theory.

VII. Appendix

Proof of Lemma 1: To simplify the notation, we assume that the sampling period is $T_S = 1$ and we restore its arbitrary value at the end. Following the definitions in Section III.A and using Eq. (6), we have for every $t, \tau \in \mathbb{R}$ that

$$R_X(t+\tau,\tau) \triangleq E\left\{x(t+\tau)x(\tau)\right\} = r_x\left([t+\tau],[\tau]\right)$$

Now we consider a fixed t and express it as $t = A + a$ where $A \in \mathbb{Z}$ and $a \in [0,1)$. Then for every integer m we have

$$\int_m^{m+1} R_X(t+\tau,\tau)\,d\tau = \int_m^{m+1} r_x\left(A+[a+\tau],[\tau]\right)d\tau = (1-a)\cdot r_x(A+m,m) + a\cdot r_x(A+m+1,m) \tag{29}$$

because it is $[a+\tau] = m$ for every $\tau \in [m, m+1-a)$ and $[a+\tau] = m+1$ for every $\tau \in [m+1-a, m+1)$. Moreover, since r_x is bounded so is R_X and so

$$\lim_{L\to\infty}\frac{1}{2L}\int_{-L}^{L} R_X(t+\tau,\tau)\,d\tau = \lim_{M\to\infty}\frac{1}{2M+1}\sum_{m=-M}^{M}\int_m^{m+1} R_X(t+\tau,\tau)\,d\tau$$

which along with Eq. (29) and the definition of $\bar{R}_x$ imply that

$$\begin{aligned}\bar{R}_x(t) &\triangleq \lim_{L\to\infty}\frac{1}{2L}\int_{-L}^{L} R_X(t+\tau,\tau)\,d\tau \\ &= (1-a)\cdot\lim_{M\to\infty}\frac{1}{2M+1}\sum_{m=-M}^{M} r_x(A+m,m) \\ &\quad + a\cdot\lim_{M\to\infty}\frac{1}{2M+1}\sum_{m=-M}^{M} r_x(A+m+1,m)\end{aligned}$$

Therefore $\bar{R}_x(t) = (1-a)\cdot\bar{r}_x(A) + a\cdot\bar{r}_x(A+1)$. Note that since $A \le t < A+1$, $\bar{R}_x(t)$ is the linear interpolation between $\bar{r}_x(A)$ and $\bar{r}_x(A+1)$ weighted by the fractional part, a, of t. Hence, in general we can write $\bar{R}_x(t)=\sum_{k=-\infty}^{\infty}\bar{r}_x(k)\operatorname{tri}(t-k)$ for every $t\in\mathbb{R}$, where $\operatorname{tri}(t)=1-|t|$ for $|t|<1$ and zero otherwise. $\bar{R}_x(t)$ can be written alternatively in the form

$$\bar{R}_x(t)=\left(\sum_{k=-\infty}^{\infty}\bar{r}_x(k)\delta(t-kT_S)\right)*\operatorname{tri}\left(\frac{t}{T_S}\right)$$

where we have also restored the value of T_S. Now, since $S_x(f)=\int_{-\infty}^{\infty}\bar{R}_x(t)e^{-2\pi ift}dt$ and the Fourier transform of the convolution equals the product of the transformations we get,

$$S_x(f)=\left(\sum_{k=-\infty}^{\infty}\bar{r}_x(k)e^{-2\pi ikf\,T_S}\right)\cdot T_S\cdot\operatorname{sinc}^2(f\cdot T_S). \qquad \square$$

Proof of Lemma 2: From Eq. (4) we calculate directly that $E\{\mathbf{x}_n\}=2G(\cos(\Omega n))-1$. Replacing G from Eq. (11) and using the property $T_j(\cos(\varphi))=\cos(j\varphi)$ of the Chebyshev polynomials, valid for every $j=0,1,2,...$ we get

$$E\{\mathbf{x}_n\}=\sum_{j=0}^{\infty}a_j\cos(\Omega nj). \tag{30}$$

Note that for $n\neq m$, random variables $\mathbf{x}_n,\mathbf{x}_m$ are independent implying that $r_x(n,m)=E\{\mathbf{x}_n\}E\{\mathbf{x}_m\}$ and so

$$r_x(n,m)=\left(\sum_{j=0}^{\infty}a_j\cos(\Omega nj)\right)\cdot\left(\sum_{\ell=0}^{\infty}a_\ell\cos(\Omega m\ell)\right) \tag{31}$$

To proceed further we need the series in (30) to converge sufficiently fast. Our assumption that $G\in C^2([-1,1])$ implies[10] $a_\ell=o(1/\ell^2)$, [42] and so series (30) is *absolutely* convergent implying that the Cauchy product of the two series in Eq. (31) converges (absolutely) to $r_x(n,m)$, [43], therefore

$$r_x(n,m)=\sum_{p=0}^{\infty}\left(\sum_{q=0}^{p}a_q a_{p-q}\cos(\Omega nq)\cos(\Omega m(p-q))\right). \tag{32}$$

Consider the case $n\neq m$ and express $n=k+m$ with $k\neq 0$. Then Eq. (32) becomes

$$r_x(k+m,m)=\sum_{p=0}^{\infty}c_p(k,m) \tag{33}$$

where

$$\begin{aligned}c_p(k,m)=&\frac{1}{2}\sum_{q=0}^{p}a_q a_{p-q}\cos(\Omega kq+\Omega mp)\\&+\frac{1}{2}\sum_{q=0}^{p}a_q a_{p-q}\cos(\Omega kq+\Omega m(2q-p))\end{aligned}.$$

By the definition of $\bar{r}_x$ in Eq. (9) we have

$$\begin{aligned}\bar{r}_x(k)&=\lim_{M\to\infty}\frac{1}{2M+1}\sum_{m=-M}^{M}r_x(k+m,m)\\&=\lim_{M\to\infty}\frac{1}{2M+1}\sum_{m=-M}^{M}\sum_{p=0}^{\infty}c_p(k,m)\\&=\lim_{M\to\infty}\sum_{p=0}^{\infty}\left(\frac{1}{2M+1}\sum_{m=-M}^{M}c_p(k,m)\right)\end{aligned} \tag{34}$$

Since $a_\ell=o(1/\ell^2)$ there exists a fixed number A such that for $p=1,2,3,...$ it is $|c_p(k,m)|<A/p^2$ for every $k,m\in\mathbb{Z}$ and so $\left|\frac{1}{2M+1}\sum_{m=-M}^{M}c_p(k,m)\right|<A/p^2$ for every $k\in\mathbb{Z}$ and $M=1,2,3,...$ as well. This implies the *uniform* convergence of $\sum_{p=0}^{\infty}\left(\frac{1}{2M+1}\sum_{m=-M}^{M}c_p(k,m)\right)$ with respect to k,M, [43]. Moreover,

$$\lim_{M\to\infty}\frac{1}{2M+1}\sum_{m=-M}^{M}c_p(k,m)=\begin{cases}a_0^2 & \text{if } p=0\\ \dfrac{a_{(p/2)}^2}{2}\cos\left(\dfrac{\Omega kp}{2}\right) & \text{if } p=2,4,6,...\\ 0 & \text{otherwise}\end{cases}$$

where the only terms of $c_p(k,m)$ remaining after taking the limit $M\to\infty$ are the ones independent of m. The uniform convergence and the existence of the limit for every $k\in\mathbb{Z}$ allow us to interchange the order of the limit and the infinite sum in the last expression of $\bar{r}_x(k)$ in Eq. (34), i.e.,

$$\bar{r}_x(k)=\sum_{p=0}^{\infty}\left(\lim_{M\to\infty}\frac{1}{2M+1}\sum_{m=-M}^{M}c_p(k,m)\right) \tag{35}$$

Therefore, for $k\neq 0$ it is $\bar{r}_x(k)=a_0^2+\frac{1}{2}\cdot\sum_{\ell=1}^{\infty}a_\ell^2\cos(\Omega k\ell)$. Finally for $k=0$ it is $r_x(m,m)=E\{\mathbf{x}_m\mathbf{x}_m\}=1$. Combining the results we express $\bar{r}_x$, using the discrete-time Dirac function δ_k, as

$$\bar{r}_x(k)=a_0{}^2+\frac{1}{2}\sum_{j=1}^{\infty}a_j{}^2\cos(j\Omega k)+\left(1-a_0{}^2-\frac{1}{2}\sum_{j=1}^{\infty}a_j{}^2\right)\cdot\delta_k \qquad \square$$

Proof of Lemma 3: The DTFT of: $\cos(j\Omega k)$, constant function 1 and Dirac function δ_k are $\pi\sum_{k=-\infty}^{\infty}\delta(\omega\pm j\Omega-2\pi k)$, $2\pi\sum_{k=-\infty}^{\infty}\delta(\omega-2\pi k)$ and 1 respectively [47]. Therefore, the DTFT of the average autocorrelation function in (15) is

$$\begin{aligned}s_x(\omega)\;=\;&\frac{\pi}{2}\sum_{j=1}^{\infty}a_j{}^2\sum_{k=-\infty}^{\infty}\delta(\omega-2\pi k\pm j\Omega)\\&+2\pi\,a_0{}^2\sum_{k=-\infty}^{\infty}\delta(\omega-2\pi k)+\left(1-a_0{}^2-\frac{1}{2}\sum_{j=1}^{\infty}a_j{}^2\right)\end{aligned}$$

Replacing $\omega=2\pi f T_S$ and using the identity of the Dirac δ function, $\delta(Mx)=\delta(x)/|M|$, we get

[10] Milder conditions, sufficient for proving Lemma 2, exist.

$$s_x\left(2\pi f T_S\right) = \frac{1}{4T_S}\sum_{j=1}^{\infty} a_j^{\,2} \sum_{k=-\infty}^{\infty} \delta\left(f - \frac{k}{T_S} \pm \frac{j\Omega}{2\pi T_S}\right) + \frac{a_0^{\,2}}{T_S}\sum_{k=-\infty}^{\infty}\delta\left(f - \frac{k}{T_S}\right) + \left(1 - a_0^{\,2} - \frac{1}{2}\sum_{j=1}^{\infty} a_j^{\,2}\right) \tag{36}$$

resulting in $T_S \cdot s_x\left(2\pi f T_S\right) = S_H(f) + S_N(f) + S_0(f)$ where the three components $S_H(f)$, $S_N(f)$ and $S_0(f)$ are given by expressions (17), (18) and (19) respectively. □

Proof of Theorem 1: From $S_H(f)$ in Lemma 3 we get that

$$4S_H(f) = \sum_{j=-\infty}^{\infty}\sum_{k=-\infty}^{\infty} a_{|j|}^2 \delta\left(f - \frac{jw+kq}{qT_S}\right) - a_0^2 \sum_{k=-\infty}^{\infty}\delta\left(f - \frac{k}{T_S}\right) \tag{37}$$

Since $\gcd(w,q)=1$ there exists an integer solution (j_1,k_1) of the Diophantine equation $wj_1 + qk_1 = 1$, [46]. Now consider the mapping from $\mathbb{Z}^2$ to itself such that $\begin{bmatrix} j \\ k\end{bmatrix} = \begin{bmatrix} j_1 & q \\ k_1 & -w\end{bmatrix}\cdot\begin{bmatrix} h \\ r\end{bmatrix}$ which is bijective because $\det\begin{bmatrix} j_1 & q \\ k_1 & -w\end{bmatrix} = -1$. Therefore we can replace the indices in the summations of (37) yielding $\sum_{j=-\infty}^{\infty}\sum_{k=-\infty}^{\infty} a_{|j|}^2 \delta\left(f - \frac{jw+kq}{qT_S}\right) = \sum_{h=-\infty}^{\infty}\delta\left(f - f_h\right)\sum_{r=-\infty}^{\infty} a_{I(h,r)}^2$ where we have set $I(h,r) = \left|j_1 h + qr\right|$, $f_h = h/\left(qT_S\right)$ and used the equation $wj_1 + qk_1 = 1$. Coefficients $b_h \triangleq \sum_{r=-\infty}^{\infty} a_{I(h,r)}^2$ are well defined because $a_\ell = o\left(1/\ell^2\right)$ (see the proof of Lemma 2) and so the series converges. Note that $I(-h,r) = I(h,-r)$ gives $b_{-h} = b_h$ which along with $f_{-h} = -f_h$ imply $\sum_{h=-\infty}^{\infty}\delta\left(f - f_h\right) b_h = \sum_{h=1}^{\infty} b_h\left(\delta\left(f - f_h\right) + \delta\left(f + f_h\right)\right) + b_0\delta(f)$. Combining it with the intermediate results and Eq. (37) yields

$$S_H(f) = \frac{1}{4}\sum_{h=1}^{\infty} b_h\left(\delta\left(f - f_h\right) + \delta\left(f + f_h\right)\right) + \frac{b_0}{4}\delta(f) - \frac{a_0^2}{4}\sum_{k=-\infty}^{\infty}\delta\left(f - \frac{k}{T_S}\right) \tag{38}$$

Adding $S_0(f)$ from expression (19) to (38) we get that

$$S_H(f) + S_0(f) = \frac{1}{4}\sum_{h=1}^{\infty} b_h\left(\delta\left(f - f_h\right) + \delta\left(f + f_h\right)\right) + \frac{3a_0^2}{4}\sum_{k=1}^{\infty}\left(\delta\left(f - \frac{k}{T_S}\right) + \delta\left(f + \frac{k}{T_S}\right)\right) + \frac{b_0 + 3a_0^2}{4}\delta(f)$$

and so $S_H(f) + S_0(f) = \tilde{S}_H(f) + \tilde{S}_0(f)$ where $\tilde{S}_H(f)$ and $\tilde{S}_0(f)$ are defined in Eqs. (22) and (23) respectively. □

Proof of Lemma 4: For every $k \in \mathbb{Z}$ and $h = 0,1,2,\ldots$ we have that $b_{kq+h} = \sum_{r=-\infty}^{\infty} a_{I(kq+h,r)}^2 = \sum_{r=-\infty}^{\infty} a_{I(kq+h,r-j_1 k)}^2$ and since $I\left(kq+h, r - j_1 k\right) = I(h,r)$ we conclude $b_{kq+h} = b_h$. Similarly we have that $b_{\ell q - h} = \sum_{r=-\infty}^{\infty} a_{I(\ell q - h, r)}^2 = \sum_{r=-\infty}^{\infty} a_{I(\ell q - h, -r - j_1 \ell)}^2$ and since $I\left(\ell q - h, -r - j_1 \ell\right) = I(h,r)$ it is $b_{\ell q - h} = b_h$. Using them along with the fact that $h - \left(h \bmod q\right)$ is always a multiple of q we get that $b_h = b_{h \bmod q} = b_{q - (h \bmod q)}$. □

Proof of Lemma 6: For $h = 0,1,2,\ldots,[q/2]$ we define the set of integers $\mathbf{I}_h \triangleq \left\{\left| j_1 h + qr\right| \mid r \in \mathbb{Z}\right\}$ and so we can write

$$b_h = \sum_{j \in \mathbf{I}_h} a_j^2 . \tag{39}$$

We first show that sets $\mathbf{I}_h$ form a partition of $\{0,1,2,\ldots\}$, i.e.,

$$\{0,1,2,\ldots\} = \bigcup_{h=0,1,\ldots,[q/2]}^{\oplus} \mathbf{I}_h \tag{40}$$

Since $wj_1 + qk_1 = 1$, it is $\gcd\left(j_1, q\right) = 1$, [46], and so for every $j \in \{0,1,2,\ldots\}$ there exist $h \in \{0,1,2,\ldots,q-1\}$ and $r \in \mathbb{Z}$ such that $j_1 h + qr = j$. If $h > [q/2]$ then it is $\left|j_1 h' + qr'\right| = j$ for $h' = q - h$ and $r' = -j_1 - r$. Therefore $\{0,1,2,\ldots\} = \bigcup_{h=0}^{[q/2]} \mathbf{I}_h$. Now let $h, h' \in \{0,1,2,\ldots,[q/2]\}$ and $r, r' \in \mathbb{Z}$, and suppose that $\left|j_1 h + qr\right| = \left|j_1 h' + qr'\right|$. If $j_1 h + qr = j_1 h' + qr'$ then $j_1\left(h - h'\right)$ is a multiple of q and since $\gcd\left(j_1, q\right) = 1$, q must divide $h - h'$ implying that $h = h'$. Similarly, if $j_1 h + qr = -\left(j_1 h' + qr'\right)$ then $j_1\left(h + h'\right)$ is a multiple of q and so q must divide $h + h'$ which is possible only if $h = h' = 0$ or $h = h' = q/2$ when q is even. In all cases it must be $h = h'$ and so the sets $\mathbf{I}_h$, $h = 0,1,2,\ldots,[q/2]$ are mutually disjoint. Lemma 4 implies that $b_h = 0$ for every $h \in \{0,1,2,\ldots\} - \mathbf{H}$ if and only if $b_h = 0$ for every $h \in \{0,1,2,\ldots[q/2]\} - \{0,w\}$. Because of Eqs. (39), (40) the last one is equivalent to having $a_j = 0$ for every $j \in \{0,1,2,\ldots\} - \mathbf{I}_0 - \mathbf{I}_w$. Using $wj_1 + qk_1 = 1$ we write $\left|j_1 w + qr\right| = \left|j_1 w + k_1 q - k_1 q + qr\right| = \left|1 + \left(r - k_1\right) q\right|$ and so $\mathbf{I}_w = \left\{1, rq \pm 1 \mid r = 1,2,3\ldots\right\}$. Also, $\mathbf{I}_0 = \left\{rq \mid r = 0,1,2,\ldots\right\}$ and so we have $\mathbf{I}_0 \bigcup \mathbf{I}_w = \mathbf{J}$ which concludes the proof. □

ACKNOWLEDGMENT

The authors would like to thank Mr. Kostas Galanopoulos of the National Technical University of Athens, Greece for the insightful discussions.

REFERENCES

[1] R.B. Staszewski, “State-of-the-art and future directions of high-performance all-digital frequency synthesis in nanometer CMOS”, IEEE Trans. *Cir. and Sys. I, Vol.* 58, Iss. 7, 2011, pp. 1497-1510.

[2] R. B. Staszewski, P.T. Balsara, *All-Digital Frequency Synthesizer in Deep-Submicron CMOS*, Wiley, John & Sons, 2006.
[3] R.B. Staszewski, et al., "All-digital PLL and transmitter for mobile phones", IEEE *Solid-State Cir., J., vol.* 40, no.12, 2005, pp. 2469-2482.
[4] R.B. Staszewski, et al., "All-digital TX frequency synthesizer and discrete-time receiver for Bluetooth radio in 130-nm CMOS", IEEE *Solid-State Cir., J., vol.* 39, no. 12, 2004, pp. 2278-2291.
[5] R.B. Staszewski, P.T. Balsara, "Phase-domain all-digital phase-locked loop", IEEE Trans. *Circ. and Sys. II, Vol.* 52, Iss. 3, 2005, pp. 159-163.
[6] I.L. Syllaios, R.B. Staszewski, P.T. Balsara, "Time-domain modeling of an RF all-digital PLL", IEEE Trans. *Circ. and Syst. II, Vol.* 55, Iss. 6, 2008, pp. 601-605.
[7] E. Temporiti, C. Weltin-Wu, D. Baldi, R. Tonietto, F. Svelto, "A 3 GHz fractional all-digital PLL with a 1.8 MHz bandwidth implementing spur reduction techniques", IEEE *Solid-State Cir. Journal 44*(3), 824-834.
[8] V. Kratyuk, P.K. Hanumolu, U.K. Moon, K. Mayaram, "A design procedure for all-digital phase-locked loops based on a charge-pump phase-locked-loop analogy." Circuits and Systems II: Express Briefs, IEEE Transactions on 54.3 (2007): 247-251.
[9] R. Tonietto, E. Zuffetti, R.Castello, I. Bietti, "A 3MHz bandwidth low noise RF all digital PLL with 12ps resolution time to digital converter", European Solid-State Circ. Conf. (ESSCIRC) 2006, pp. 150-153.
[10] L. Fanori, A. Liscidini, R. Castello, "3.3 GHz DCO with a frequency resolution of 150Hz for All-digital PLL", *IEEE Solid-State Cir. Conf. (ISSCC), 2010*, pp. 48-49.
[11] K. Hosseini and M. P. Kennedy, "Maximum sequence length MASH digital delta—sigma modulators," IEEE Trans. Circuits Syst. I, Reg. Papers, vol. 54, no. 12, pp. 2628–2638, Dec. 2007.
[12] H. Mair and L. Xiu, "An architecture of high-performance frequency and phase synthesis," IEEE J. Solid-State Circuits, vol. 35, no. 6, pp. 835–846, Jun. 2000.
[13] L. Xiu, "The concept of time-average-frequency and mathematical analysis of flying-adder frequency synthesis architecture," IEEE Circuits Syst. Mag., vol. 8, no. 3, pp. 27–51, 3rd Quart., 2008.
[14] L. Xiu, W. Li, J. Meiners, and R. Padakanti, "A novel all digital phase lock loop with software adaptive filter," IEEE Journal of Solid-State Circuit, vol. 39, no. 3, pp. 476–483, Mar. 2004.
[15] L. Xiu, "Nanometer Frequency Synthesis beyond Phase Locked Loop," August 2012, John Wiley IEEE press.
[16] L. Xiu, W. T. Lin and K. Lee, "A Flying-Adder Fractional-Divider based integer-N PLL: the 2nd generation Flying-Adder PLL as clock generator for SoC", IEEE J. Solid-State Circuits, vol. 48, pp.441-455, Feb. 2013.
[17] P. Sotiriadis, "Theory of flying-adder frequency synthesizers part I: Modeling, signals periods and output average frequency," IEEE Trans. Circuits Syst. I, vol. 57, no. 8, pp. 1935–1948, Aug. 2010.
[18] P. Sotiriadis, "Theory of flying-adder frequency synthesizers part II: Time and frequency domain properties of the output signal," IEEE Trans. Circuits Syst. I, vol. 57, no. 8, pp. 1949–1963, Aug. 2010.
[19] P. Sotiriadis, "Exact Spectrum and Time-Domain Output of Flying-Adder Frequency Synthesizers", IEEE Trans. on Ultrasonics, Ferr., and Frequency Control, Vol. 57, No. 9, Sep. 2010, pp. 1926-1935.
[20] B. Pontikakis, H.-T. Bui, F.-R. Boyer, and Y. Savaria, "Precise freerunning period synthesizer (FRPS) with process and temperature compensation", IEEE MidWest Symp. Circ. Syst., 2007, pp. 1118–1121.
[21] D. E. Calbaza and Y. Savaria, "A direct digital periodic synthesis circuit," IEEE J. Solid-State Circ., vol. 37, no. 8, pp. 1039–1045, 2002.
[22] F. L. Martin, R. E. Stengel, and J.-K. Juan, "Method and apparatus for digital frequency synthesis," U.S. Patent 6 891 420, filled: Dec 21, 2001, Motorola, Inc.
[23] K. Galanopoulos, P. Sotiriadis, "Optimal Dithering Sequences for Spurs Suppression in Pulse Direct Digital Synthesizers", IEEE International Frequency Control Symposium, May 2012, pp. 1-4.
[24] K. Galanopoulos, P. Sotiriadis, "Modulation Techniques for All-Digital Transmitters Based on Pulse Direct Digital Synthesizers", IEEE International Frequency Control Symposium, May 2012, pp. 1-4.
[25] E. McCune, "Direct digital frequency synthesizer with designable stepsize," in Proc. IEEE Radio Wireless Symp. (RWS) , Jan. 2010.
[26] T. Gradishar, R. Stengel, "Method and apparatus for noise shaping in direct digital synthesis", US Patent 7,143,125, filled: Apr. 16, 2003, assignee: Motorola, Inc., IL, USA.
[27] H. Nosaka, Y. Yamaguchi, A. Yamagishi, H. Fukuyama, and M. Muraguchi, "A Low-Power Direct Digital Synthesizer Using a Self-Adjusting Phase-Interpolation Technique", IEEE J. Solid-State Circuits, Vol. 36, no. 8, 2001, pp. 1281-1285.
[28] H. Tucholski, "Direct digital synthesizer with output signal jitter reduction", US Patent 7,103,622, filed: Oct. 8, 2002, assignee: Analog Devices, Inc., Norwood, MA, USA.
[29] J. Rode, A. Swaminathan, I. Galton, and P. M. Asbeck, "Fractional-N direct digital frequency synthesis with a 1-bit output," in IEEE MTT-S Int. Microw. Symp. Dig., Jun. 2006, pp. 415–418.
[30] Paul P. Sotiriadis, Kostas Galanopoulos, "Direct All-Digital Frequency Synthesis techniques, Spurs Suppression and Deterministic Jitter Correction", IEEE Trans. on Circuits and Systems-I, Volume: 59 , Issue: 5, Pages: 958 – 968, May 2012.
[31] J. Vankka and K. Halonen, *Direct Digital Synthesizers: Theory, Design and Applications*, New york, Springer 2006.
[32] J. Tierney, C. M. Radar, and B. Gold, "A digital frequency synthesizer," IEEE Trans. Audio Electroacoust., vol. AC-19, pp. 48–57, Mar. 1971.
[33] U.L. Rohde, *Microwave and Wireless Synthesizers: Theory and Design*, 1st ed. Singapore: Wiley-Interscience, 1997.
[34] V.S. Reinhardt, "Direct digital synthesizers", Technical Report, Hughes Aircraft Co, Space and Communications Group, L.A., CA, Dec. 1985.
[35] C. E. Wheatley, III, "Digital frequency synthesizer with random jittering for reducing discrete spectral spurs," U.S. Patent 4410954, Oct. 1983.
[36] V. N. Kochemasov and A. N. Fadeev, "Digital-computer synthesizers of two-level signals with phase-error compensation," Telecommun. Radio Eng., vol. 36/37, pp. 55–59, Oct. 1982.
[37] R.M. Gray, "Quantization noise spectra", *IEEE Trans. Information Theory, Vol.* 36, Iss. 6, 1990, pp. 1220-1244.
[38] B. Widrow, I. Kollar, M.-C. Liu. "Statistical theory of quantization." *IEEE Trans. Instrum. and Measur., Vol.* 45, no. 2, 1996, pp. 353-361.
[39] J.G. Proakis, M. Salehi, *Digital Communications*, 5th Ed., McGraw-Hill Companies,Inc. , 2007.
[40] R.M. Gray, "Quantization noise spectra", *IEEE Trans. Information Theory, Vol.* 36, Iss. 6, 1990, pp. 1220-1244.
[41] J.P. Boyd, *Chebyshev and Fourier Spectral Methods*, Dover Publications, 2nd Ed., 2001.
[42] G.H. Hardy, W.W. Rogosinski, *Fourier Series*, Dover Public., 1956.
[43] J. M. Hyslop, *Infinite Series*, Dover Publications 2006.
[44] W. Kester (Editor), *Data Conversion Handbook* (Analog Devices), Newnes 2005.
[45] J.C. Candy (Ed.), G.C. Temes (Ed.), *Oversampling Delta-Sigma Data Converters: Theory, Design, and Simulation*, Wiley-IEEE Press, 1991.
[46] D. E. Flath, *Introduction to Number Theory*. New York: Wiley, 1989.
[47] A.V. Oppenheim, R.W. Schafer, J.R. Buck, *Discrete-time signal processing*, Prentice Hall, N. Jersey, 2nd Edition, 1999
[48] A. Zygmund, *Trigonometric Series,3rd Ed.* , Cambridge Un. Press 2003.

Paul P. Sotiriadis (Senior IEEE member) received the Ph.D. degree in electrical engineering and computer science from the Massachusetts Institute of Technology in 2002, the M.S. degree in electrical engineering from Stanford University, Stanford, CA, and the Diploma degree in electrical and computer engineering from the National Technical University of Athens, Greece. In 2002, he joined the Johns Hopkins University as Assistant Professor of Electrical and Computer Engineering. In 2012, he joined the faculty of the Electrical and Computer Engineering Department of the National Technical University of Athens, Greece.

He has authored and coauthored 85 technical papers most of them in IEEE journals and conferences, holds one patent, has several patents pending, and has contributed chapters to technical books. His research interests include the design, optimization, and mathematical modeling of analog, mixed-signal and RF integrated and discrete circuits, advanced frequency synthesis, biomedical instrumentation, and interconnect networks in deep-submicrometer technologies. He has led several projects in these fields funded by U.S. organizations and has collaborations with industry and national labs.

He has received several awards, including the 2012 Guillemin-Cauer Award from the IEEE Circuits and Systems Society, best paper award in the IEEE Int. Frequency Control Symp. 2012, and best paper award in the IEEE Int. Symp. on Circuits and Systems 2007. Dr. Sotiriadis is an Associate Editor of the IEEE Sensors Journal, has served as an Associate Editor of the IEEE Trans. on Circuits and Systems-II from 2005 to 2010 and has been a member of technical committees of many conferences. He regularly reviews for many IEEE transactions and conferences and serves on proposal review panels.

Natalia Miliou (member IEEE) received the Diploma and M.S. degrees (summa cum laude) in Electrical Engineering and Computer Technology from the University of Patras, Greece in 2002, and the Ph.D. degree in Information

Technology and Electrical Engineering from the Swiss Federal Institute of Technology (ETH), Zurich, Switzerland, in 2007, where she was a member of the Signal and Information Processing Laboratory. In 2005-2006 she was a visiting researcher at the Laboratory for Information and Decision Systems (LIDS) of the Massachusetts Institute of Technology (MIT) working on Network Coding for Wireless Networks.

Between 2008 and 2012 she was involved in several European research projects as an information and communication theory expert. She is currently a research fellow at the Electrical and Computer Engineering Department, National Technical University of Athens, Greece.

Dr. Miliou's interests are in the general area of information theory, communication theory, signal processing and their applications. She regularly reviews for IEEE transactions on Information Theory, Wireless Communications, Physical Communication (Elsevier), Advances in Electronics and Telecommunications, as well as for numerous IEEE conferences including ISIT, Globecom, DYSPAN, PIMRC, and she has been in the technical program committees of a number of conferences on wireless communications.